THE ASTROPHYSICAL JOURNAL, 403:743–751, 1993 February 1

A SPECTROSCOPIC STUDY OF DV URSAE MAJORIS (US 943), AY PISCIUM (PG 0134+070), AND V503 CYGNI

PAULA SZKODY[1]
Department of Astronomy, University of Washington, Seattle, WA 98195

AND

STEVE B. HOWELL[1,2]
Planetary Science Institute, 2421 E, 6th Street, Tucson, AZ 85719
Received 1992 May 8; accepted 1992 August 5

ABSTRACT

We have determined radial velocity solutions for the two eclipsing cataclysmic variables DV UMa and AY Psc, which yield mass estimates for the stellar components. AY Psc appears to have a high-mass white dwarf (1.3 $M_\odot$), consistent with its high rate of mass transfer and lack of a hot spot. On the other hand, DV UMa, with its orbital period below the gap, low mass transfer rate, and prominent hot spot modulation, has a low-mass (0.4 $M_\odot$) white dwarf. A low-mass white dwarf is also indicated in the ultrashort period system V503 Cyg. However, the interpretation of V503 Cyg is complicated, since it does not eclipse and the spectroscopic period differs from the period obtained using large-amplitude humps in the continuum light. Possible causes for this difference might be associated with a magnetic nonsynchronously rotating white dwarf, the existence of superhump-type phenomena, or the changing illumination of an irradiated secondary.

Subject headings: binaries: eclipsing — novae, cataclysmic variables — stars: individual (DV Ursae Majoris, AY Piscium, V503 Cygni)

1. INTRODUCTION

Our recent observational programs using time-resolved CCD photometry to determine the prominent orbital features present in faint cataclysmic variables have led to the discovery of two eclipsing systems (DV UMa = US 943; Howell et al. 1988b; and AY Psc = PG 0134+070; Szkody et al. 1989) as well as one with a very large amplitude hump modulation (V503 Cyg; Szkody et al. 1989). In order to derive the masses of the stellar components and the inclinations of the systems to the line of sight, as well as to understand the origin and contribution of the hot spot component to the system light, we have obtained time-resolved spectra of these three objects.

Several recent reviews on mass determinations for cataclysmic variables (Shafter 1991; Robinson 1992) have pointed out the difficulties of using emission-line velocity measurements to yield accurate mass determinations. In particular, distortions in the lines created by hot spots or the accretion disk may produce noticeable phase shifts of up to 0.15 phase between the time of photometric eclipse and the zero-crossing of the radial velocity curve. The understanding of these effects will come only through study of a variety of eclipsing systems with a range of orbital periods and a variety of systems with hot spots. DV UMa, AY Psc, and V503 Cyg provide a good laboratory for the study of the effect of the hot spot on the determination of system parameters. DV UMa and AY Psc both have 1.3 mag deep eclipses in V light but are contrasts in orbital period and hot spot strength, with DV UMa having a very short period (2.06 hr) and a prominent (0.7 mag amplitude) spot, while AY Psc has a relatively long orbital period (5.22 hr) with no evidence for a spot hump in the continuum. V503 Cyg does not eclipse, but has a very short orbital period (1.82 hr) and a light curve which is completely dominated by the presence of a hump modulation that has an amplitude of up to 1 mag and a duration of more than 0.5 in phase.

2. OBSERVATIONS

The spectroscopic data were obtained during two runs (1989 May 7, 8, 9 and October 18, 19) on the KPNO 4 m telescope with the RC CCD spectrograph, using grating KPC-007A in first order with a 250 μm slit (1".5), which gave a resolution of 2.7–2.9 Å and a wavelength coverage of 4250–4950 Å. On the night of October 18, simultaneous CCD photometry for V503 Cyg was obtained by B. Schaefer on the 0.9 m telescope, using the TEK1 CCD and a V filter with 120 s integrations.

Additional light curves for V503 Cyg were obtained at Lowell Observatory using the 1.8 m Perkins telescope during 1991 June. These time-series observations were made in I band on June 22 UT ($V \sim 18.01$, $I \sim 18.20$) and June 28 UT ($V \sim 17.23$, $I \sim 17.04$). The V magnitudes were obtained from a single frame just before the start of the I time series data and the I magnitudes given are the mean values (outside the humps). The listed V and I magnitudes have an error of ± 0.1 mags. We also report here on observations that were obtained during an outburst on 1982 July 24 and 25 with a photometer on the 0.76 m telescope at Manastash Ridge Observatory (MRO). A problem with the photometer prevented an accurate determination of the V magnitude on that run, but the system was obviously at outburst ($V \sim 13$; measured in comparison to nearby stars) and the relative magnitudes could be used to identify a hump feature in the light curve.

The observations for each object are summarized in Table 1.

The spectra were reduced with standard IRAF "twodspec" routines to subtract the bias, divide by the flat field, extract and subtract the sky from the spectra, followed by "onedspec" routines to obtain wavelength and flux calibrations. Line fluxes and equivalent widths were measured with the interactive e routine in "splot," which sums the line flux between continuum

[1] Visiting Astronomer, Kitt Peak National Observatory, NOAO, operated by the Association of Universities for Research in Astronomy, Inc. (AURA), under cooperative agreement with the National Science Foundation.
[2] Visiting Astronomer, Lowell Observatory.

TABLE 1

SUMMARY OF OBSERVATIONS

Object	UT Date	Exposure	Number of Spectra or Photometry	UT Time	State
DV UMa	1989 May 7	10 minutes	11	3:56–6:30	Quiescence
	1989 May 8	10 minutes	10	3:56–5:46	Quiescence
AY Psc	1989 Oct 18	15 minutes	11	7:28–12:00	Quiescence
V503 Cyg	1982 Jul 24	10 s	*U*, *B*, *V* phot	8:55–10:35	Outburst
	1982 Jul 25	10 s	*U*, *B*, *V* phot	9:31–10:32	Outburst
	1989 May 7	10 minutes	3	10:54–11:25	Superoutburst
	1989 May 8	5 minutes	18	8:57–10:48	Superoutburst
	1989 Oct 18	10 minutes	18	2:56–6:35	Quiescence
	1989 Oct 18	2 minutes	*V* phot	3:36–6:00	Quiescence
	1989 Oct 19	10 minutes	9	2:57–4:43	Quiescence
	1991 Jun 22	3 minutes	*I* phot	8:22–10:43	Quiescence
	1991 Jun 28	3 minutes	*I* phot	7:10–10:00	Outburst rise

points determined by setting a cursor on each side of the line. Velocities were determined by the e (centroid) routine, the d (one or multiple Gaussian fits) routine, and a routine that we incorporated into IRAF which is based on the double-Gaussian method of Shafter (Shafter, Szkody, & Thorstensen 1986).

The KPNO photometry was reduced using routines on the telescope computer to subtract the bias and divide by the flat field followed by the picture packing and aperture routines for differential photometry contained in "cdphot." The magnitudes of V503 Cyg and two comparison stars on the same frames were measured. The difference between the two comparison stars was constant to ± 0.01 mag throughout the photometric run. Since the two comparison stars were of roughly equal magnitude to each other and to V503 Cyg, we can take ± 0.01 mag as a measure of the precision of the differential light curve. The Lowell photometric data were measured with the IRAF "apphot" routines. Since these data were obtained in the *I* band, two different comparison stars (different from the KPNO *V* data) were used in the reductions. The error in the differential light curve data was calculated based on Howell et al. (1988a) methods and was determined to be ± 0.018 mag on both nights.

3. RESULTS

3.1. *DV Ursae Majoris*

The light curve of this faint object (Howell et al. 1988b) is normally at a mean $V \sim 19.3$ level, with a rise to a pre-eclipse hump of $V \sim 18.6$ peaking at phase 0.8 and a decrease during eclipse to $V \sim 20.6$. The low-resolution spectrum obtained on a 4.2 m telescope by Mukai et al. (1990) showed the presence of TiO bands from a late-type secondary and Hα clearly in emission, but the higher order Balmer lines were noisy. Our 10 minute spectra have low signal-to-noise ratio (S/N), but the Hβ line is clearly visible. Figure 1 shows the combined average spectrum created from the nine out-of-eclipse spectra obtained on May 8. Hβ shows the typical broad double-peaked line profile of a high inclination system. Figure 2 shows the changes that occur in the line profile at different times of the orbit. At phase 0.91 (near the peak of the hump), the line shows the narrow single-peaked component from the spot, while at phase 0.44, the line is double-peaked with the central absorption extending to the continuum level.

In order to improve the S/N for velocity measurement, we combined phases from the two nights. Unfortunately, the accuracy of the period determination of Howell et al. (1988b) did

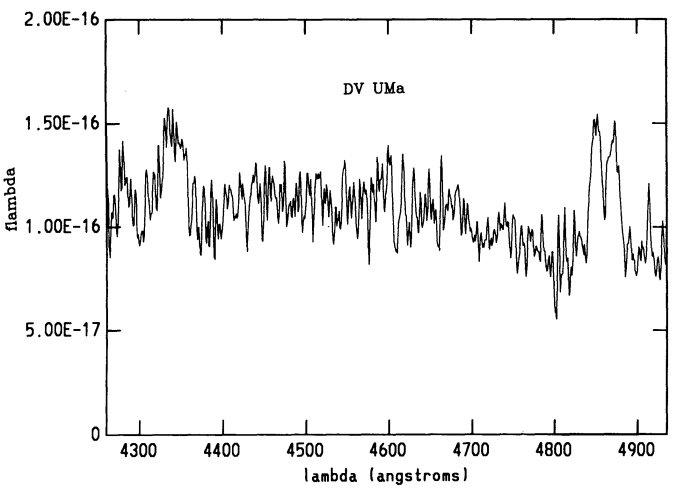

FIG. 1.—The combined out-of-eclipse spectrum of DV UMa from averaging nine spectra obtained 1989 May 8

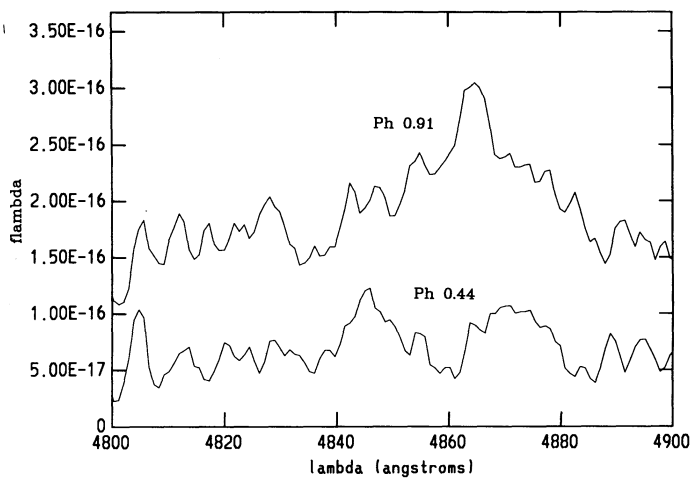

FIG. 2.—The Hβ line profile at the peak of the orbital hump (phase 0.91) compared to a midphase (0.44)

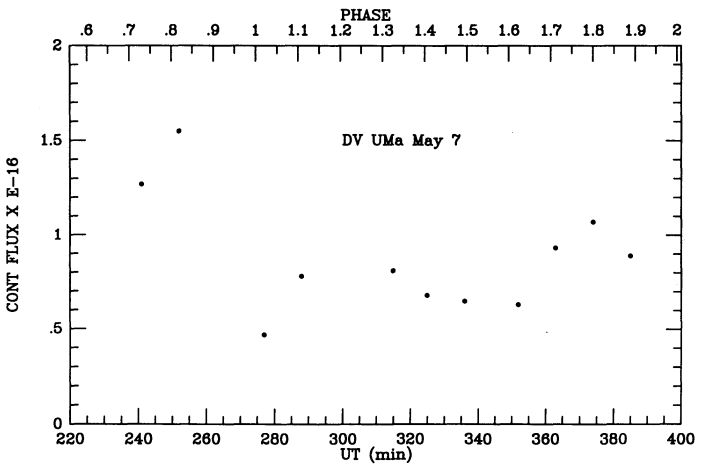

FIG. 3a

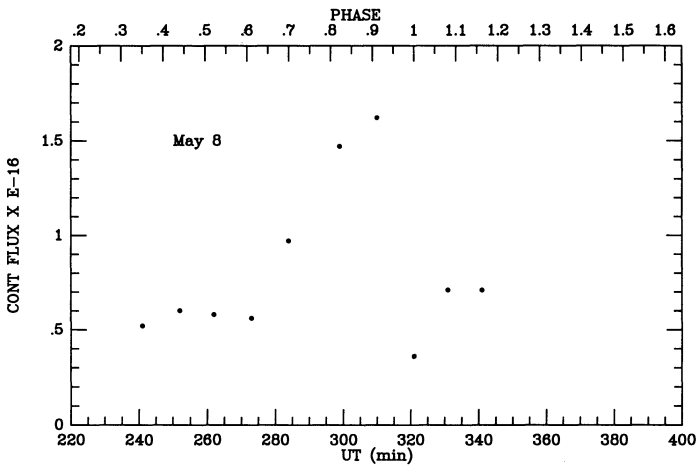

FIG. 3b

FIG. 3.—(*a*)–(*b*) The continuum flux measurements near Hβ measured from the spectra obtained May 7 and 8. The phase as determined from the eclipse on May 8 is listed at the top.

not permit us to extrapolate the ephemeris to our 1989 observations. However, the continuum flux measurements enabled us to do "slit photometry" to establish the eclipse timings. Figure 3 shows our light curves created from the continuum flux measurements of our spectra for May 7 and 8, which are very similar to the Howell et al. broad-band continuum light curves. The data on May 8 permit the most accurate determination of the eclipse time (321 minutes UT). Using the period to extrapolate back to May 7 predicts the eclipse at 275 minutes UT on that date. Figure 3 shows that this time matches with the observed light curve.

Using these eclipse times for photometric phase 0 and the period of Howell et al. (1988b) enabled us to combine subsets of the 21 spectra that were obtained within 0.04 phase of each other on the two nights. This resulted in 10 spectra, with phase bins 0.71 and 0.81 having three spectra, phase 0.16 only one spectrum, and the remainder of the phase bins having averages of two spectra. The individual and combined spectra were measured with e, d, and Shafter routines to obtain velocities. The method yielding the least scatter used a Gaussian fit to each of the two peaks in the line (except for phase 0.9 which has a single-peaked line and so a single Gaussian was used, and phase 0 where no line was detected), with the final velocity being the midpoint of the two Gaussians. The best-fit sine wave of the following form was fitted to the resulting nine velocities, and the solution is shown in Figure 4 and listed in Table 2.

$$V = \gamma - K \sin 2\pi(\phi - \phi_0) .$$

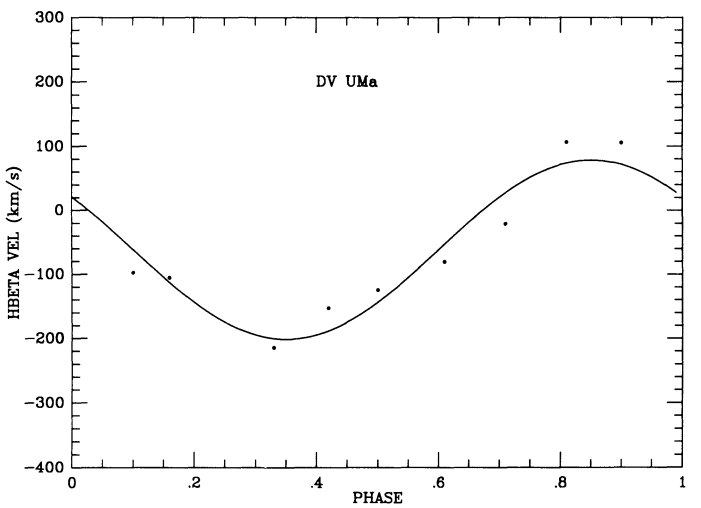

FIG. 4.—The radial velocities of the phase-combined data from May 7 and 8 along with the best fit sine-curve solution.

3.2. *AY Piscium*

The initial *B* and *V* light curves of AY Psc (Szkody et al. 1989) showed a symmetrical eclipse with no evidence of a hot spot hump preceding the eclipse. Further eclipses obtained by Diaz & Steiner (1990) provide an ephemeris that is highly accurate (better than 0.01 phase) at the epoch of our spectra. Our 11 spectra provide the first time-resolved spectroscopy of this object. Although they cover only about 0.7 of an orbit, the extrema of the positive and negative velocity excursions are covered so that a radial velocity curve may be constructed. Since the mean *V* magnitude of AY Psc is 15.8, the individual 15 minute exposures provide sufficient S/N for effective velocity measurement of Hβ. Figure 5 shows the changing line profile throughout the observations. The full width zero intensity (FWZI) of Hβ is between 30 and 40 Å. The least scatter in the velocity curve was obtained with a Shafter double-Gaussian method with 3 Å Gaussians (full width half-maximum) separated by 23 Å. The velocity solution is given in Table 2 and shown in Figure 6.

3.3. *V503 Cygni*

The three initial *V* light curves at quiescence obtained over six nights (Szkody et al. 1989) established a period of 109.42 $\pm$ 0.06 minutes, from the existence of an extremely large (0.8–1.0 mag) amplitude hump modulation, with the hump

TABLE 2

RADIAL VELOCITY SOLUTIONS FOR DV URSAE MAJORIS AND AY PISCIUM[a]

Object	γ (km s^{-1})	K (km s^{-1})	ϕ_0
DV UMa	-61 ± 13	140 ± 18	0.10 ± 0.02
AY Psc	67 ± 17	131 ± 20	0.05 ± 0.03

[a] Errors given are 1 σ.

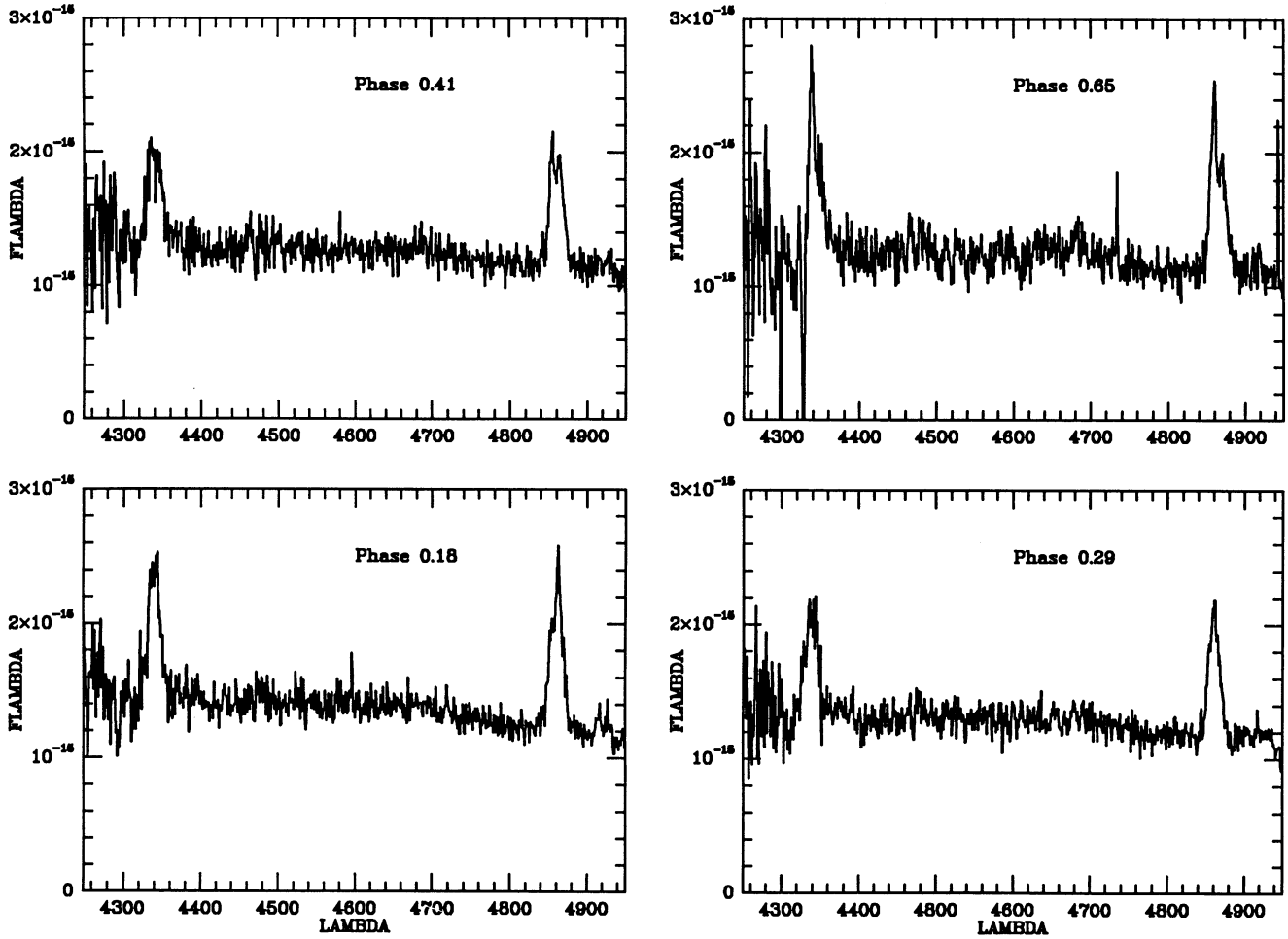

FIG. 5.—The changing line profile of AY Psc throughout most of its orbit. Note the narrow component that moves from red (phase 0.18) to blue (phase 0.65).

lasting about 70% of the orbit. The initial spectrum at quiescence (Szkody 1985) showed broad (50 Å FWZI for Hβ) but relatively weak (for a system below the period gap) Balmer lines while the colors indicated both blue ($U-B \sim -0.8$) and red ($V-J \sim 2.7$) components. The short outburst recurrence time for this dwarf nova (about 1 month) allows the chance to study this system both at outburst (mean $V \sim 13.4$) and quiescence (mean $V \sim 17.4$). Our spectroscopic data cover an outburst in 1989 May (Fig. 7) and quiescence in 1989 October (Fig. 8). A night of quiescent photometry on 1989 October 18 (Fig. 9) simultaneous with the spectroscopy allows us to match unambiguously the times of the continuum hump to the spec-

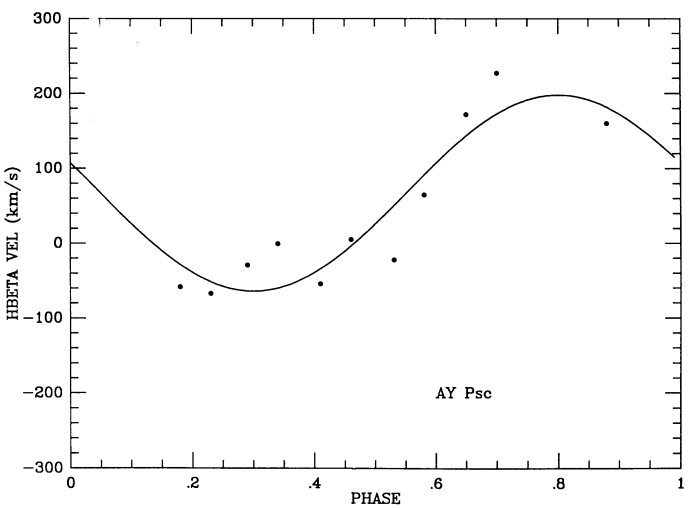

FIG. 6.—The radial velocities and best fit sine-curve solution for AY Psc

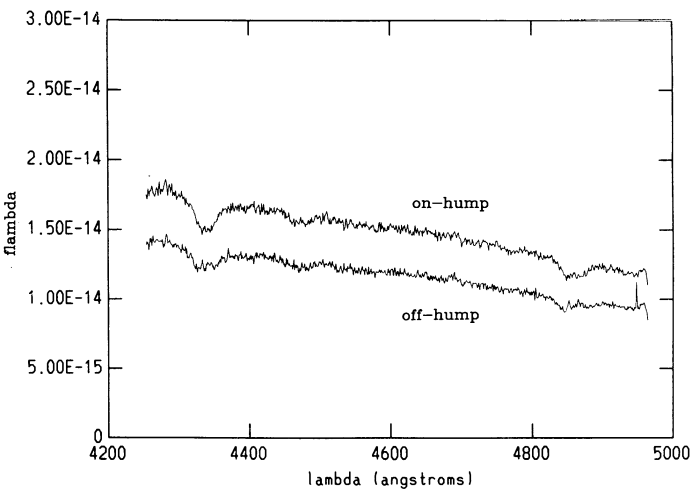

FIG. 7.—The individual spectra obtained during the peak of the hump and at minimum during the 1989 May outburst of V503 Cyg.

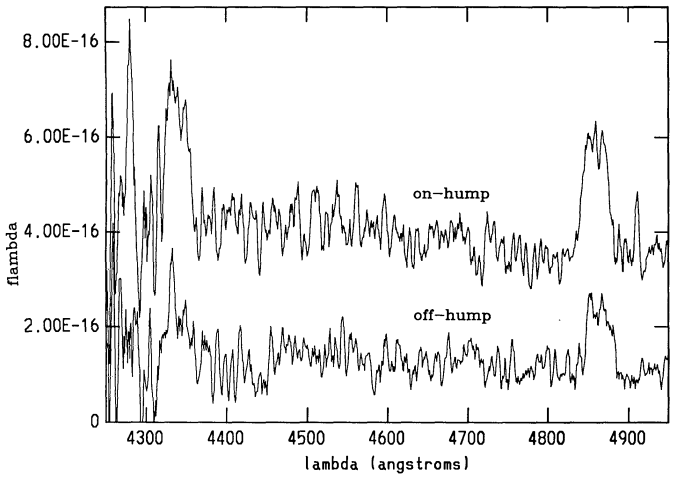

FIG. 8.—The smoothed individual spectra during the peak of the hump and at minimum during quiescence in 1989 October.

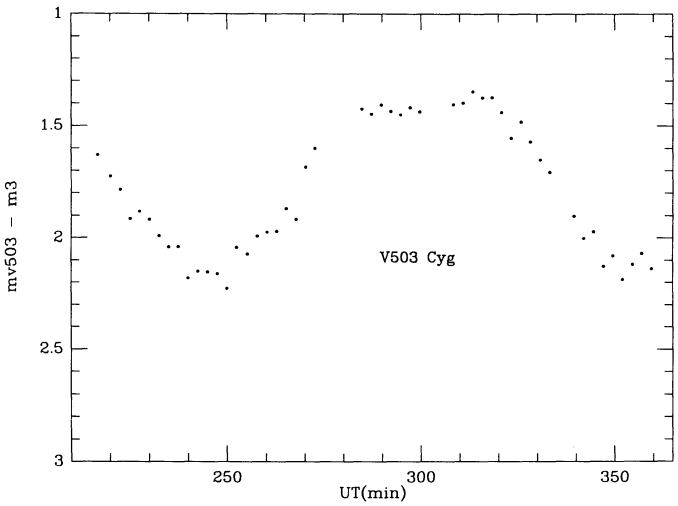

FIG. 9.—The photometric light curve obtained simultaneously with the 1989 October 18 spectroscopy. The *y*-axis is the differential *V* magnitude of V503 Cyg with respect to a nearby comparison star.

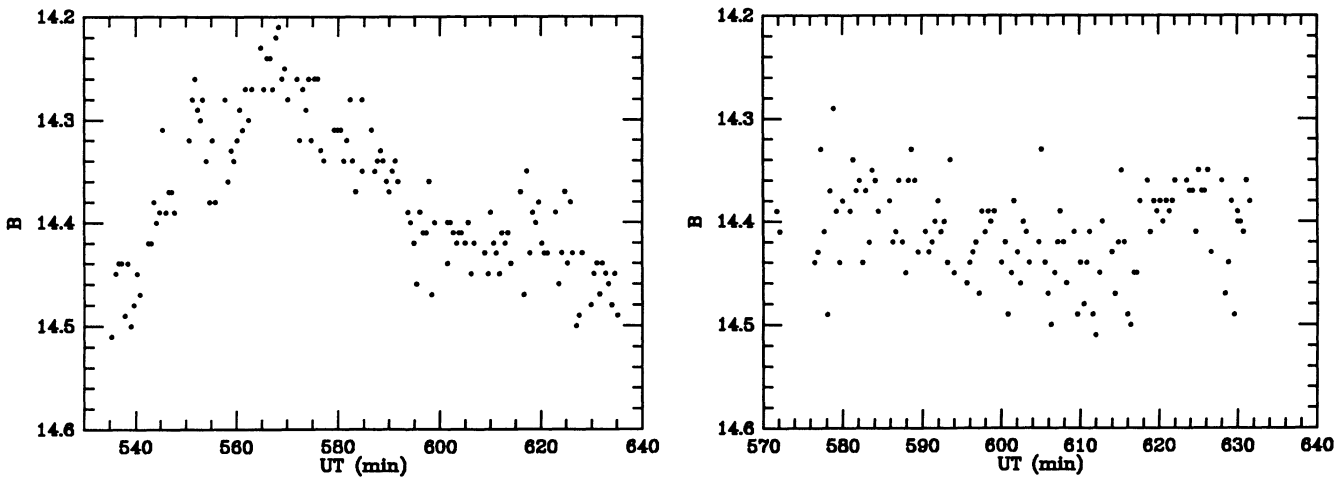

FIG. 10.—The photometric *B* light curves of V503 Cyg obtained during an outburst in 1982 July. The left panel, covering a full orbit, is July 24 and the right, covering only about half the orbit, is July 25.

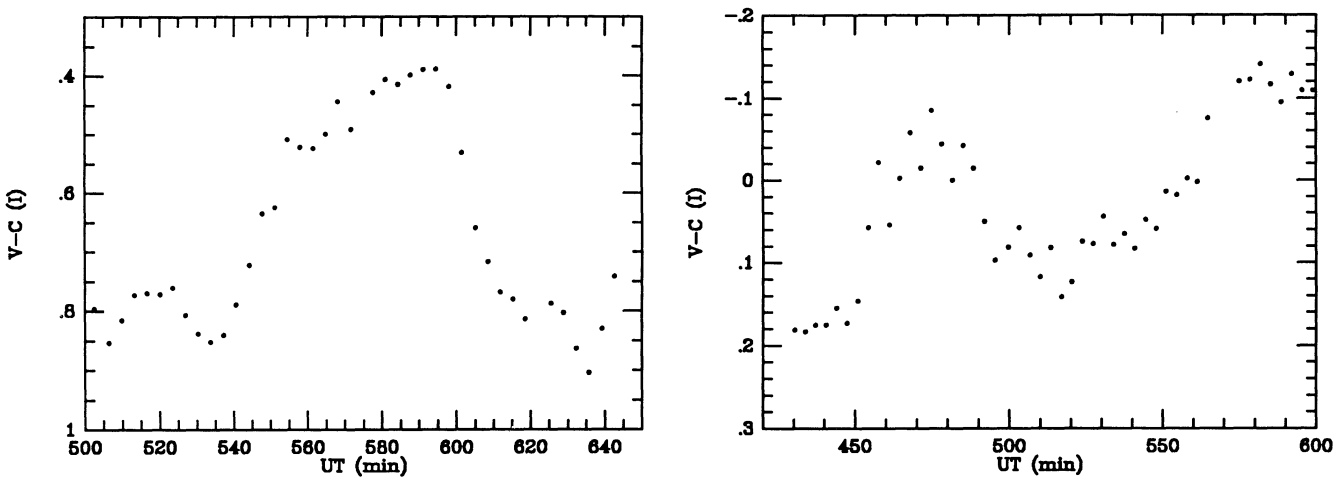

FIG. 11.—The *I* band differential light curve of V503 Cyg with respect to the same comparison star obtained at quiescence on 1991 June 22 and during the rise to outburst on 1991 June 28.

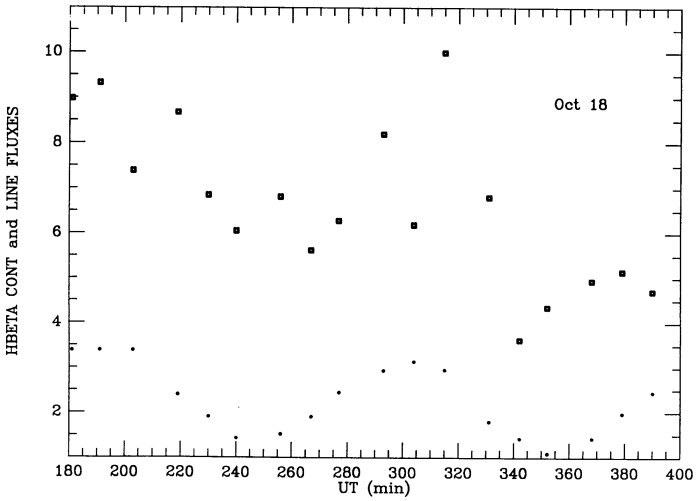

FIG. 12*a*

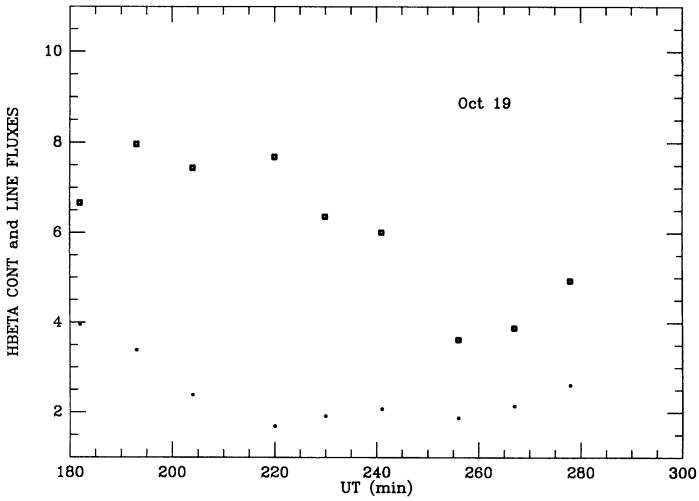

FIG. 12*b*

FIG. 12.—(*a*)–(*b*) The continuum fluxes (*dots*) in units of 10^{-16} ergs cm^{-2} s^{-1} Å^{-1} and Hβ line fluxes above the continuum (*squares*) in units of 10^{-15} ergs cm^{-2} s^{-1} measured from the spectra of 1989 Oct. 18 and 19.

troscopic behavior. Photometry during an outburst in 1982 July (Fig. 10) and during a rise to outburst in 1991 June (Fig. 11) was also obtained.

Since V503 Cyg is not eclipsing and the photometric hump period is not known well enough to extrapolate the ephemeris from Szkody et al. (1989) to the 1989 observations, the simultaneous photometry and spectroscopy provides the best opportunity to study the relation of the continuum and spectra. The continua and line fluxes of the 27 quiescent spectra from October 18 and 19 were measured and are shown in Figure 12. It can be seen that the continua flux variations clearly show the periodic hump modulation that is seen in the broad-band *V* photometry of the past 1988 data and the simultaneous October 18 *V* band data (Fig. 9). The flux change of the continuum near Hβ has a larger amplitude (1.2 mag) compared to the broad-band *V* (0.8 mag) simultaneous measurement. The line fluxes show the same general trends as the continuum but with larger scatter on October 18, while the October 19 line flux variation appears delayed by 20–30 minutes with respect to the continuum (see discussion below).

In determining the velocity curves, we tried e and Shafter methods on individual spectra and on averages based on period-folding and on combining adjacent spectra. The least scatter was obtained with the Shafter method with 5 Å (FWHM) Gaussians separated by 30 Å. Because of the decreasing S/N as higher airmass was reached during the October 18 observations, averaging the latter spectra with the earlier ones by phase produced more scatter than combining adjacent spectra. Thus, the best results were obtained by applying a running average to the spectra (i.e., averaging the first and second, then the second and third, etc.). This gave 17 measurements for October 18 and eight for October 19. The measured velocities and the best-fit sine curve with the period fixed at 109.42 minutes are shown in Figure 13. The fits and one σ errors are listed in Table 3.

While the fits on the two nights are consistent with each other, the errors became larger when a combined solution for both nights was tried (Table 3). The reason for this discrepancy becomes obvious when considering the velocity curves as a function of the 109.42 minute period. On October 18, the most negative velocities occur near 210 and 320 UT. With a period of 109.42 minute, the velocity minimum for October 19 *should* occur at 193 UT, yet Figure 13*b* shows it occurs at 227 UT, a delay of 34 minutes! Inspection of Figure 12 shows that the continuum variation follows the photometric period of 109.42 (hump maxima near 191 and 300 UT on October 18 and at the predicted time of 173 UT on October 19). If the continuum fluxes were delayed by 34 minutes, the hump maximum would occur near 207 minutes. While this is obviously *not* the case for the continuum variation, the line fluxes *do* peak near 207 minutes. Thus we are led to the conclusion that the lines follow a different period than the continuum. If the period is left as a

TABLE 3

RADIAL VELOCITY SOLUTIONS FOR V503 CYGNI

Date (1989)	Number of Points	γ (km s^{-1})	K (km s^{-1})	t_0	P (minutes)
Oct 18	17	15 ± 14	137 ± 20	185 ± 3	109.42 (fixed)
Oct 18	17	13 ± 15	138 ± 20	187 ± 4	107 ± 4
Oct 19	8	−30 ± 09	131 ± 13	200 ± 2	109.42 (fixed)
Oct 18, 19	25	−4 ± 19	87 ± 26	193 ± 5	109.42 (fixed)
Oct 18, 19	25	−4 ± 11	137 ± 16	190 ± 2	103.7 ± 0.3
May 8	17	38 ± 16	124 ± 23	431 ± 3	109.42 (fixed)
May 8	17	35 ± 15	140 ± 22	452 ± 9	94 ± 6
May 7, 8	20	60 ± 21	116 ± 31	436 ± 4	109.42 (fixed)
May 7, 8	20	44 ± 15	140 ± 20	433 ± 3	107.0 ± 0.8

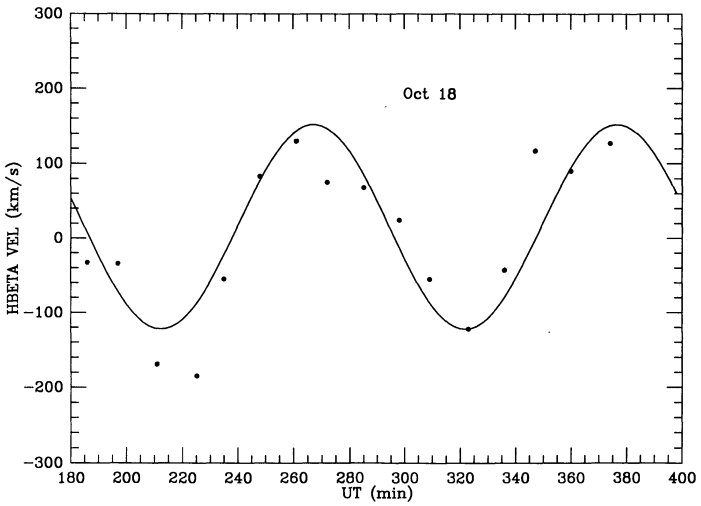

FIG. 13*a*

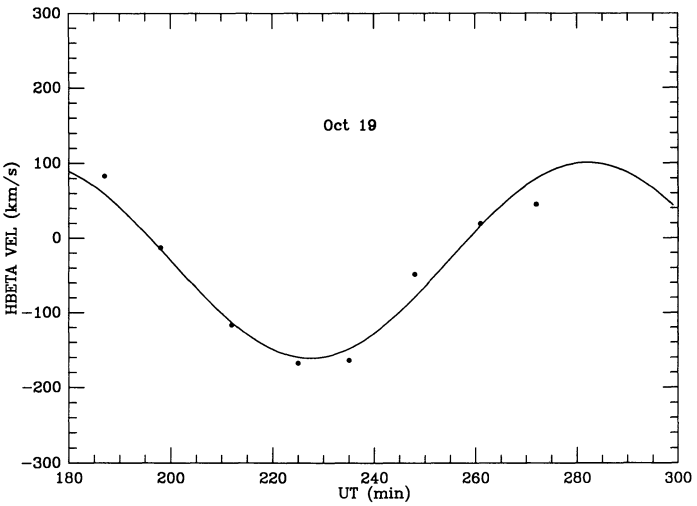

FIG. 13*b*

FIG. 13.—(*a*)–(*b*) The radial velocities and best fit sine-curve solutions determined with the period fixed at 109.42 min

free parameter in the velocity solution for the combined October 18 and 19 data, the solution improves and the resulting period determination is 103.7 ± 0.3 minutes (Table 3).

We can use the simultaneous photometry and spectroscopy from October 18 to attempt to determine the origin of the line radiation relative to the continuum. Figures 9 and 12*a* compared to Figure 13*a* show that the peak of the continuum hump comes at the red to blue crossing of the radial velocity curve. In a typical cataclysmic variable, phase 0 is defined as the red to blue crossing for the emission lines which originate in the disk close to the white dwarf component. For this scenario to explain a large increase in the continuum light, the inclination would have to be low enough (<66°) so that the secondary did not eclipse the white dwarf/inner disk, and the side of the disk between the white dwarf and the secondary would have to be bright (perhaps by the impact of the stream). However, most streams impact offset from the line of centers, due to the angular momentum, and they usually produce a narrow *S*-wave component in the emission lines (e.g., as is seen in the short-period binary SW UMa; Shafter et al. 1986).

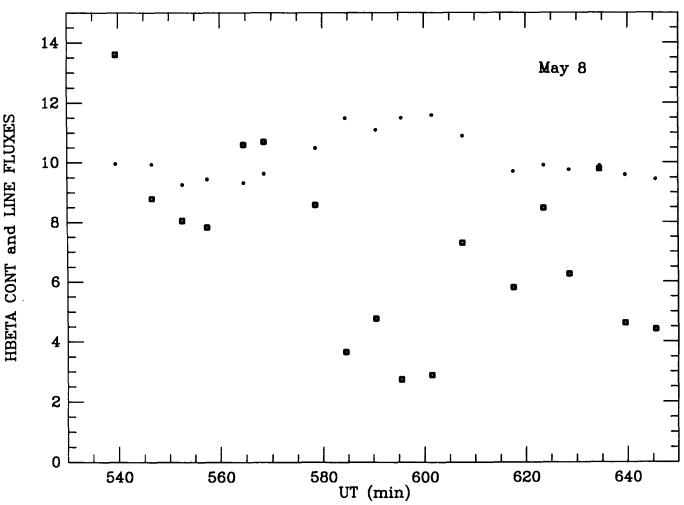

FIG. 14.—The continuum (*dots*) in units of 10^{-15} ergs cm^{-2} s^{-1} Å^{-1} and Hβ line fluxes above the continuum (*squares*) in units of 10^{-15} ergs cm^{-2} s^{-1} measured from the outburst spectra of 1989 May 8.

The other possibility is that the origin of the line emission is from the secondary, which is heated on the side facing the white dwarf. Thus the red to blue crossing of the secondary would correspond to viewing the heated side (phase 0.5 or inferior conjunction of the white dwarf in the usual terminology). While this provides a more natural explanation for the large continuum hump, it is difficult to reconcile the different period of the line flux and velocity variation for the two nights combined. On October 19, the peak continuum flux comes just after maximum positive velocity.

In order to test the validity of the difference in continuum and spectroscopic periods, we turned to the outburst data of 1989 May. The continuum measurements from the slit spectra (Fig. 14) show a hump behavior, although the amplitude is less (0.2 mag) and the width is narrower than the hump seen at quiescence. The presence of a hump at outburst is confirmed by the MRO data, obtained at outburst (Fig. 10) and the Lowell data (Fig. 11), obtained during the rise. In the latter case, the hump timings for the single hump on June 22 and the two observed on June 28 are consistent with a period of 109.42 minutes. All known hump maxima and minima (which are narrower and hence possibly easier to measure accurately) at the current time are listed in Table 4.

Figure 7 shows that the Balmer emission is just a weak feature in the core of broad absorption at outburst, which is typical of spectra obtained during dwarf novae outbursts. When the line flux of this weak emission is measured, it is anticorrelated with the hump feature in the continuum (Fig. 14). The emission line is too weak for velocity measurement,

TABLE 4

TIMINGS FOR V503 CYGNI (JD 2,440,000+)

Date	Maxima	Minima
1982 Jul 24	5174.896	5174.927
1988 Sep 14	7418.818	7418.856
1988 Sep 15	7419.803	7419.845
1988 Sep 19	7423.682, 7423.757	7423.647, 7423.720, 7423.796
1989 May 8	7654.913	...
1989 Oct 18	7817.633, 7817.708	7817.672, 7817.749
1989 Oct 19	...	7818.660
1991 Jun 22	8429.902	8429.860, 8429.935
1991 Jun 28	8435.830, 8435.906	8435.860

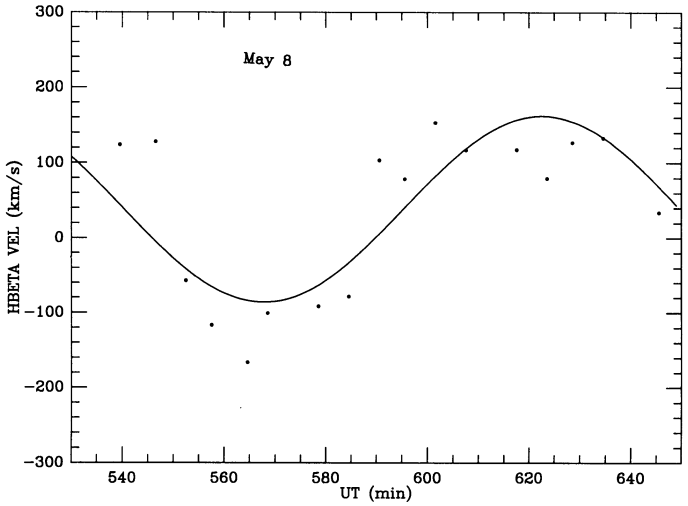

FIG. 15.—The radial velocities and best fit sine-curve solution for the May 8 broad absorption line of Hβ, with the period fixed at 109.42 minutes.

but the broad absorption could be measured. A double Gaussian Shafter method with 4 Å wide Gaussians separated by 40 Å gave the least scatter and the velocity solution and data are shown in Figure 15 and stated in Table 3. In this case, the hump maximum (590 UT in Fig. 14) occurs at the blue to red crossing of the velocity curve (opposite to the quiescent data). This is consistent with an origin of the broad absorption from the accretion disk near the white dwarf, and the hump continuum from the irradiated secondary. If the hump at maximum is the same hump as at quiescence, this lends confirmation to the hump source on the irradiated secondary. However, ultrashort period dwarf novae can show superhumps during some outbursts, which have a different period and origin from the normal hot spot hump seen at quiescence. The AAVSO records (Mattei 1992) indicate that the 1989 May outburst was a superoutburst, lasting for 9 days. It is impossible to determine from the available data whether the hump seen on May 8 (Fig. 14) is a superhump or the normal hump at quiescence overwhelmed by the brighter disk luminosity. Comparison of Figures 12 and 14 shows that the continuum is brighter by about a factor of 10 at outburst from quiescence, so the 1.2 mag hump amplitude apparent in Figure 12 would be about a 0.3 mag hump amplitude in Figure 14. This is close to what is observed. It is also in the range of the typical superhump amplitudes observed in other short-period systems (Warner 1985a).

Although there are only three spectra available for the night of May 7, a similar result was obtained from combining the data for the May 7 and 8 nights as in combining the quiescent data over two nights; i.e., the solution improves if the period is not fixed at 109.42 minutes and the spectroscopically determined period is shorter than the photometric period. In the case of superhumps (Warner 1985a), the superhump period is always a few percent *longer* that the orbital period. Recent theoretical ideas to explain the superhump involve a periodic stressing and dissipation in a precessing eccentric disk (Vogt 1982; Whitehurst 1988; Osaki 1989). However, to obtain a superoutburst, the models require $q < 0.25$ (which does not appear to be the case for V503 Cyg; see section below). In addition, there are no known systems where the superhumps persist at quiescence. Models to explain different periodicities at quiescence generally involve magnetic phenomena, where one period is the spin period of the white dwarf and the longer period is usually the orbital period (Berriman 1988). However, in V503 Cyg, the orbital period as determined by the spectroscopic solution, is the *shorter* period. This object may be similar to the old nova CP Pup, which has a photometric modulation of 1.59 hr and a spectroscopic radial velocity period of 1.47 hr (Vogt et al. 1990). Although the amplitude of the photometric modulation is much lower (0.15 mag) in CP Pup than in V503 Cyg, the extent of the modulation is similar (Warner 1985b).

4. MASS DETERMINATIONS

For eclipsing systems, the mass of the secondary M_s, the mass ratio of the secondary to the primary q, and the inclination of the system to the line of sight may be determined from three equations (the following are taken from eqs. [4], [5], and [7] of Downes et al. 1986):

$$M_s^2 = 0.996 \times 10^{-8} P^2 (q + 1/q)(0.462[q/q + 1]^{1/3})^3 \beta^3 M_\odot ,$$

$$M_s = K_{wd}^3 P(q + 1/q)^2/2\pi G \sin^3 i ,$$

$$[0.462(q/q + 1)^{1/3}]^2 \beta^2 = \cos^2 i + \sin^2 i \sin^2 (2\pi\phi_{1/2}) .$$

In the case of V503 Cyg, which is not eclipsing, the solution for the inclination comes from the following equation (Shafter 1981):

$$\sin i = 3.79 \times 10^{-3} K(1 + 1/q)^{2/3} P^{-0.055} ,$$

$$K/v_d \sin i = q(0.5 - 0.227 \log q)^2 .$$

The values used and the results obtained for the primary and secondary masses and inclinations are summarized in Table 5. The uncertainty of 20 km s^{-1} in the amplitudes (Tables 2 and 3) results in the largest uncertainties in the mass ratio and primary masses (0.15–0.20 in q and 0.1–0.3 $M_\odot$), with smaller uncertainties in inclination and secondary masses (5° and 0.02 $M_\odot$). In addition, there will be some uncertainties associated with the problems described by Shafter (1991) and Robinson (1992). Despite not knowing the white dwarf masses to a few tenths, it is possible to determine if the systems contain massive or low-mass primaries. The results in Table 5 show a large range, with a very massive white dwarf in AY Psc and a very

TABLE 5

SYSTEM PARAMETERS

Object	K (km s^{-1})	P (s)	$\phi_{1/2}$[a]	$V_d \sin i$ (km s^{-1})	M_s	M_{wd}	q	i°
AY Psc	131	18776.5	0.024	...	0.59	1.31	0.45	74
DV UMa	140	7428	0.017	...	0.23	0.43	0.54	72
V503 Cyg	140	6565	...	534	0.2	0.2	1.0	55

[a] $\phi_{1/2}$ is the orbital phase where the eclipsed object's light is reduced by 50%.

low mass white dwarf in V503 Cyg. The overall results are consistent with the photometric properties of each system. AY Psc has no offset between the photometric and spectroscopic solutions (Table 2), consistent with no major distortion of the light curve by the hot spot. In this relatively long period system, the disk is large, resulting in a short infall distance for the stream and a low bright spot luminosity (Lin 1975). In addition, the high white dwarf mass contributes to a high disk luminosity so the spot luminosity is a small proportion of the total light. On the other hand, DV UMa, with a short orbital period, has a prominent orbital hump from a hot spot and a 0.1 phase offset from the photometric eclipse phase. This is consistent with the greater infall distance for the smaller disk, giving a higher spot luminosity which is prominently seen in comparison to a low-luminosity disk surrounding the low-mass white dwarf.

The last case, V503 Cyg, has a mass ratio of 1. This could explain why the radial velocity amplitudes are identical when the system is at outburst (the absorption lines used to construct the velocity curve likely originate from the disk close to the white dwarf) and when the system is at quiescence (when the velocity curve is constructed from emission lines which might originate from the secondary). However, if this is the correct interpretation of the sources of emission, the difference in period between the photometric humps and the spectroscopic period still needs to be explained.

5. CONCLUSIONS

The evidence for a high-mass white dwarf in the longer period nova-like AY Psc which has no noticeable orbital hot spot modulation, and for a low-mass white dwarf in the short-period dwarf nova system DV UMa, which has a very prominent hot spot modulation, corroborates the ideas expressed by Bailey (1990) and Webbink (1990) that the mean white dwarf mass may increase with orbital period, and by Shafter (1991), that there is a tendency for phase shifts to be more pronounced at short orbital period.

However, the short-period dwarf nova V503 Cyg, with a very prominent orbital modulation, presents a major puzzle. The similar radial velocity amplitude from the emission lines at quiescence and the absorption lines at outburst result in a very low white dwarf mass, consistent with the above. But the phasing of the peak of the continuum flux with respect to the velocity curve changes by 180° between quiescence and outburst. While this would be consistent with an origin of the quiescent emission lines from the irradiated secondary and of the outburst absorption lines from the disk, the apparent difference in period between the continuum modulation and the spectroscopic velocity modulation seen on nightly time scales means that the (continuum) hot spot cannot remain at a fixed location during orbital time scales. Possible models for explaining this type of phenomena include magnetic white dwarfs whose spin is not synchronized to the orbit, secondaries irradiated by a precessing disk which changes the illumination zone, and superhump type models invoking eccentric disks. Of these ideas, the superhump explanation has problems with the amplitude and presence of the modulation at quiescence, the magnetic model is unusual with the orbital (spectroscopic) period being shorter than the photometric period, and the irradiated secondary model has difficulties with the large displacements needed on short time scales. This same type of problem is present in the old nova CP Pup, although its modulation is of lower amplitude.

It is clear that we do not yet understand all the perturbations that may occur to produce hot spots in short-period systems. In the case of V503 Cyg, progress may be made in the understanding of the physical cause of the hot spot modulation by obtaining X-ray fluxes (to determine the high-energy radiation that is available to produce irradiation of the secondary), by obtaining circular polarization data (to explore the existence of a strongly magnetic white dwarf), and by monitoring the orbital and spectroscopic periods through several days and through an outburst (to determine the changes to the photometric modulation as the disk brightens).

We gratefully acknowledge Brad Schaefer for enthusiastically obtaining and reducing the simultaneous photometry of V503 Cyg on October 18. This work was partially supported under NSF grants AST 89-15445 and AST 89-14866. PSI is a nonprofit division of SAIC. This is PSI contribution number 297.

REFERENCES

Bailey, J. 1990, MNRAS, 243, 57
Berriman, G. 1988, in Polarized Radiation of Circumstellar Origin, ed. G. V. Coyne et al. (Vatican City State: Vatican Observatory), 105
Diaz, M. P., & Steiner, J. E. 1990, A&A, 238, 170
Downes, R. A., Mateo, M., Szkody, P., Jenner, D., & Margon, B. 1986, ApJ, 301, 240
Howell, S. B., Mason, K. O., Reichert, G. A., Warnock, A., & Kreidl, T. J. 1988b, MNRAS, 233, 79
Howell, S. B., Mitchell, K. J., & Warnock, A. W. 1988a, AJ, 95, 247
Lin, D. N. C. 1975, MNRAS, 170, 379
Mattei, J. 1992, private communication
Mukai, K., et al. 1990, MNRAS, 245, 385
Osaki, Y. 1989, PASJ, 41, 1005
Robinson, E. L. 1992, in Vina del Mar Workshop on Cataclysmic Variable Stars, ed. N. Vogt (ASP Conf. Series), 3
Shafter, A. W. 1991, in Proc. 12th North American Workshop on Cataclysmic Variables, ed. A. W. Shafter, San Diego State University, 39
Shafter, A. W., Szkody, P., & Thorstensen, J. 1986, ApJ, 308, 765
Szkody, P. 1985, AJ, 90, 1837
Szkody, P., Howell, S. B., Mateo, M., & Kreidl, T. J. 1989, PASP, 101, 899
Vogt, N. 1982, ApJ, 252, 653
Vogt, N., Barrera, L. H., Barwig, H., & Mantel, K.-H. 1990, in Accretion-Powered Compact Binaries, ed. C. W. Mauche (Cambridge: Cambridge Univ. Press), 391
Warner, B. 1985a, Interacting Binaries, ed. P. Eggleton & J. Pringle (Dordrecht: Reidel), 367
———. 1985b, MNRAS, 127, 1
Webbink, R. 1990, in Accretion-Powered Compact Binaries, ed. C. W. Mauch (Cambridge: Cambridge Univ. Press), 177
Whitehurst, R. 1988, MNRAS, 232, 35